

ELE438—Lab Report

Lee Taylor

December 2025

Contents

1 Modelling	2
1.1 First Order Input Response	2
1.1.1 Model Derivation	2
1.1.2 Experiment on the Real System	2
1.2 Minor Model Improvements	3
2 Control Design	4

1 Modelling

1.1 First Order Input Response

The original LTI model of the helicopter assumes control of the elevation and pitch rates ($\dot{E}(t)$ and $\dot{\Psi}(t)$) as if the steady-state fan force at a given input is applied instantaneously, this is not the case in the real system as the fans have a finite response time.

1.1.1 Model Derivation

New states $V_a(t)$ and $V_b(t)$ were added to represent the *actual inputs*, each modelled as a first order response with unit gain and time constant τ_F equal to that of the fans' first order approximation—this was determined with system identification on the dynamic response load cell data to be $\tau_F = 0.87\text{s}$. In the combined model, the new states substitute for the terms involving $U_{a,b}(t)$, and control inputs are applied exclusively to them rather than on the pitch and elevation rates. This yields the combined LTI model ($x = x(t)$, $u = u(t)$, $y = y(t)$ for compactness)

$$\dot{\bar{x}} = \bar{A}\bar{x} + \bar{B}u, \quad y = C\bar{x} + Du$$

where the modified elements denoted by $\bar{\cdot}$ are

$$\bar{x} = [E \ \Psi \ \Theta \ \dot{E} \ \dot{\Psi} \ \dot{\Theta} \ V_a \ V_b]^T,$$

$$\bar{A} = \begin{bmatrix} 0 & 0 & 0 & 1 & 0 & 0 & 0 & 0 \\ 0 & 0 & 0 & 0 & 1 & 0 & 0 & 0 \\ 0 & 0 & 0 & 0 & 0 & 1 & 0 & 0 \\ -\frac{k_E}{J_E} & 0 & 0 & -\frac{c_E}{J_E} & 0 & 0 & \frac{l_1 \alpha k_a}{J_E} & \frac{l_1 \alpha k_a}{J_E} \\ 0 & -\frac{k_P}{J_\Psi} & 0 & 0 & -\frac{c_P}{J_\Psi} & 0 & \frac{l_2 \alpha k_a}{J_\Psi} & -\frac{l_2 \alpha k_a}{J_\Psi} \\ 0 & \frac{-2l_1(\alpha k_a V_e + \beta)}{J_\Theta} & 0 & 0 & 0 & -\frac{c_T}{J_\Theta} & 0 & 0 \\ 0 & 0 & 0 & 0 & 0 & 0 & -\frac{1}{\tau_F} & 0 \\ 0 & 0 & 0 & 0 & 0 & 0 & 0 & -\frac{1}{\tau_F} \end{bmatrix}, \quad \bar{B} = \begin{bmatrix} 0 & 0 \\ 0 & 0 \\ 0 & 0 \\ 0 & 0 \\ 0 & 0 \\ 0 & 0 \\ \frac{1}{\tau_F} & 0 \\ 0 & \frac{1}{\tau_F} \end{bmatrix}$$

With $V_e = U_e$. Note that spring and damping coefficients have been added to the elevation axis, as well as damping only to the travel axis, following this the notation for the spring coefficients is k_x , and damping c_x .

An equivalent method for this modification is to make the additional states the fan forces $F_{a,b}$, rather than delayed inputs, this was experimented with. In that case, the original model in Mini Assignment 1—before the $(\alpha k_a U_{a,b} + \beta)$ substitution—is used, and the fan model is taken directly from the system identification step. The reason that the current method was opted for was to make the approximation of the linear steady-state response better, allowing for a nonzero y -intercept, and to take the average across the fans' range rather than from a single measurement of the dynamic response—in the case of the direct system identification model, the linear response is only parameterised by the gain, missing out on the flexibility afforded by the β term.

1.1.2 Experiment on the Real System

To demonstrate the improvement in comparison to the original, an experiment was designed using the real helicopter pitch axis. As opposed to an experiment involving the other axes, the pitch axis alone is ideal because:

- The modelled pitch axis dynamics do not depend on the other axes

- The modelled dynamics are linear (unlike the other two)
- It can be easily isolated by holding the other two axes still
- The amount of compounding model mismatch is minimal as the fans are rigidly attached to the axis.

If the model is improved, the simulated response should match real response more closely than the original model.

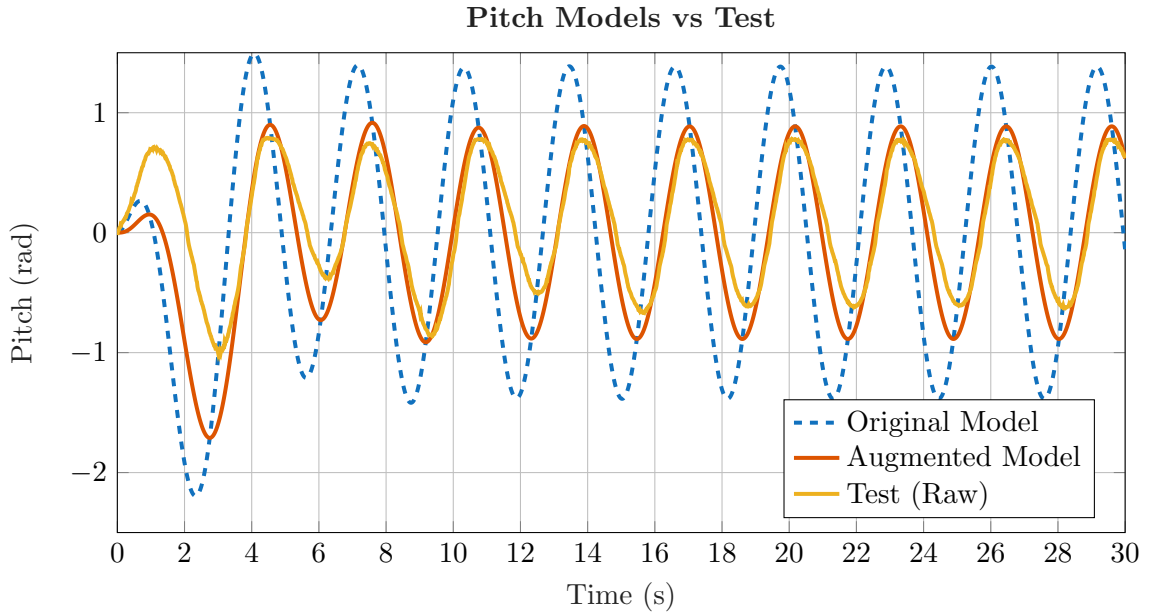


Figure 1: Pitch axis experimental data with augmented model vs old model

During the experiment, sine and cosine inputs were applied to the helicopter (with the fans out of phase with each other) to oscillate the pitch axis. The amplitude of the input signals were in the range [0.3, 10] to eliminate the nonlinear fan behaviour below the voltage threshold, the frequency of the signals is 2 rad/s—this was determined manually to get a response that spanned a large portion of the pitch axis. Using the same series of inputs, the response from each linear model was simulated. Figure 1 illustrates the simulated responses in comparison to the test data.

The MSE of the original model response was 0.8358, and the MSE of the new model was 0.0945—this shows a marked improvement. Since the other axes are functions of the pitch axis, it is a reasonable conclusion that the accuracy of the model is improved overall.

1.2 Minor Model Improvements

In the original material, the inertia of the travel axis, J_Θ , was assumed equal to the inertia of the elevation axis, $J_E = 2m_1l_1^2 + m_2l_3^2$. The equation of the inertia given a set of point masses, m_i and their distances to the axis, l_i , is $\sum m_il_i^2$. At the level hover condition, looking along the travel axis, the distance from a fan with mass m_1 , is $l_F = \sqrt{l_1^2 + l_2^2}$. This resolves to $J_\Theta = 2m_1l_1^2 + 2m_1l_2^2 + m_2l_3^2$, which has an extra term.

As briefly mentioned prior, spring and damping effects were added to the elevation and travel axes. To converge on a set of spring and damping coefficients (for all axes), a test output log—during normal controlled operation—was used to compare against a script simulation using the logged inputs. The simulation implemented nonlinear dynamics through a MATLAB function handle and 4th-order Runge-Kutta integration.

2 Control Design

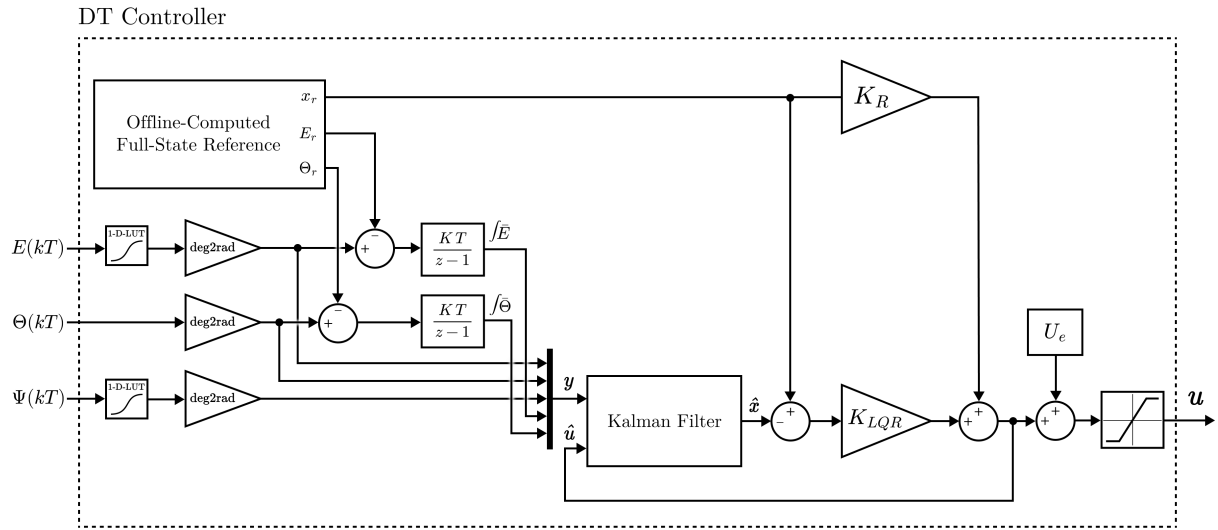


Figure 2: Controller block diagram

Figure 2 shows the controller block diagram in the dashed box.